



Photocatalytic degradation of azo pyridone dye: Optimization using response surface methodology

Jasmina Dostanić^a, Davor Lončarević^{a,*}, Ljiljana Rožić^a, Srđan Petrović^a, Dušan Mijin^b, Dušan M. Jovanović^a

^aDepartment of Catalysis and Chemical Engineering, University of Belgrade, Institute of Chemistry, Technology and Metallurgy, Njegoševa 12, 11000, Belgrade, Republic of Serbia

Tel. +381 11 2630 213; Fax: +381 11 2637 977; email: dloncarevic@nanosys.ihtm.bg.ac.rs

^bFaculty of Technology and Metallurgy, University of Belgrade, Karnegijeva 4, 11000, Belgrade, Republic of Serbia

Received 26 April 2012; Accepted 4 September 2012

ABSTRACT

Response surface methodology (RSM) and central composite design have been applied to describe and optimize photocatalytic degradation of azo pyridone dye using TiO₂, H₂O₂, and simulated sun light. The mutual interactions between three independent variables, viz. H₂O₂ concentration, irradiation time, and TiO₂ content were obtained. The results revealed that the most influential variables under selected reaction conditions were irradiation time and TiO₂ content. The optimized conditions for the photocatalytic degradation of azo pyridone dye were as follows: H₂O₂ concentration: 130.5 mg/L, irradiation time: 54.8 min, and TiO₂ content: 2.48 g/L. Under these conditions, the maximum decolorization efficiency of 96.43% was achieved. This experimental value was in good agreement with the predicted one, which proved the validity of the model. Operation cost analysis indicated that irradiation time had the major influence on total process cost. The RSM based on the central composite design was shown to be a successful technique for the optimization of the decolorization efficiency of azo pyridone dye and can be very helpful in improving the process economic feasibility. TOC analysis showed that the dye could be effectively mineralized during photocatalytic degradation.

Keywords: Photodegradation; Azo pyridone dye; Response surface methodology; Central composite design; Optimization

1. Introduction

Textile industry has been condemned as being one of the most polluting industries in the world. During the textile manufacturing processes, a large amount of wastewater containing dyestuffs with intensive color and toxicity is introduced into the aquatic systems, thus affecting aquatic life. Among the different types of dyes used in textile industries, 60–70% is azo com-

pound [1]. In anaerobic conditions, azo dyes may be resolving into potentially carcinogenic aromatic amines [2]. Therefore, in the last decades an increased attention has been given to the removal of dyes from textile effluents. Typical techniques include the classical methods such as adsorption, coagulation and ion flotation, and sedimentation [3,4]. All these techniques are versatile and useful, but they all end up in producing secondary waste products, which needs to be processed further. In the recent years, heterogeneous

*Corresponding author.

photochemical processes have become very popular as an alternative or a complement to the classical water and wastewater treatment methods [5]. The heterogeneous photocatalytic process consists in illumination of particles of semiconducting materials, such as TiO_2 , with light energy higher than their band gap energy, resulting in appearance of excited high energy states of electron and holes pairs that can migrate to the surface of the particles and initiate a wide range of redox reactions. The key advantage of this method is that it can be carried out under ambient conditions (with atmospheric oxygen as oxidant), no secondary products are produced, and may lead to complete mineralization of organic carbon to CO_2 [6].

When photocatalytic methods are used, it is desirable to have knowledge of the process variables and their influence on dye degradation in order to maximize the dye removal efficiency. A number of studies investigate effects of various parameters, i.e. initial catalyst concentration, initial dye concentration, temperature, pH, H_2O_2 concentration etc. on contaminants removal [7,8]. In most research, it has been found that the addition of H_2O_2 can improve photocatalytic degradation of different pollutants. In his work, Toor et al. [9] examined the influence of H_2O_2 on photocatalytic degradation of Direct Yellow 12 dye using UV/ TiO_2 . The authors found that there is an optimal H_2O_2 concentration where maximal decolorization efficiency is observed. Also, in a number of research experiments, it was found that the maximum decolorization rate was observed with $C(\text{H}_2\text{O}_2)/C_0$ (dye) molar ratio ranging from 10 to 100 and that further increase in H_2O_2 concentration inhibited photocatalytic degradation [10,11]. The authors stated that when present at a low concentration, H_2O_2 acts as a source of hydroxyl radicals and as an electron scavenger, thus inhibiting electron-hole recombination. At higher concentrations, H_2O_2 reacts with hydroxyl radicals, and acts as scavenger of photoproducted holes which results in decrease in the photocatalytic efficiency [12].

The majority of studies that investigate the influence of process parameters on photocatalytic degradation are performed using the conventional univariate approach, in which one parameter is varied, while the others are kept constant. This methodology can be inadequate for process optimization, since some of process parameters involve synergetic effects, as a result of interactions between variables. In addition, univariate methodology requires many experiment runs, it is time consuming, and does not necessarily allow effective optimization of the process [13].

The limitations of the univariate optimization process can be overcome through the use of statistical experimental designs, particularly response surface

methodology (RSM). RSM is very useful for designing experiments, building models, evaluating the effects of the several independent variables and searching optimum conditions for desirable responses. The main advantage of RSM is the reduced number of experimental trials needed to find optimum conditions for desirable responses [14–17].

In this study, photocatalytic degradation of azo pyridone dye using TiO_2 and simulated sun light was investigated. The optimization of the reaction parameters for the photodegradation of azo pyridone dye was performed by RSM and experimental design. The decolorization efficiency was selected as the response for optimization and functional relationship between the response and the independent variables (H_2O_2 concentration, irradiation time, and TiO_2 content) was established by means of experimental design. In addition, in order to check process economic feasibility and to find the major cost factors, the model was used for predicting operating cost of the process.

2. Experimental

2.1. Materials

Titanium dioxide was kindly supplied by Evonik Degussa GmbH (Aeroxide TiO_2 P25, 80% anatase–20% rutile, surface area – $50\text{ m}^2/\text{g}$, mean diameter — approximately 30 nm). All other chemicals were purchased from Sigma Aldrich and were of analytic reagent grade. Distilled water was used in all experiments.

The azo pyridone dye 5-(4-sulpho phenylazo)-6-hydroxy-4-methyl-3-cyano-2-pyridone was synthesized by the diazotization – coupling reaction and involves the conversion of 4-sulphoaniline to the intermediate 4-sulphobenzendiazonium ion, followed by the reaction with 3-cyano-6-hydroxy-4-methyl-2-pyridone. A detail description of dye synthesis and its structure confirmation were reported elsewhere [7].

2.2. Photocatalytic tests

The photocatalytic degradation of synthesized dye was performed in an open Pyrex beaker ($V=250\text{ mL}$, $D=67\text{ mm}$) thermostated at 25°C . In all experiments, 100 mL of aqueous suspensions, containing predefined amounts of TiO_2 and dye were magnetically stirred, so that TiO_2 can be uniformly dispersed. The concentration of dye solution was 20 mg/L and pH was 6.8.

Hydrogen peroxide was added at the beginning of each experimental run. Concentration of H_2O_2 was in the range 19–221 mg/L. In order to achieve maximum adsorption of the dye, the reaction mixture was first left for 30 min in the dark and then irradiated with the lamp (Osram Vitalux, 300 W) that simulates sun

light. The maximum intensity of lamp was in UV-(A, B, C) regions and at wavelength of 365 nm, 420 nm, 560 nm, and 580 nm. An array of 16 lamps per square meter at a distance of about 50 cm between the bulb crown and the irradiated object achieves a similar radiance as solar. The lamp was placed 50 cm above the surface of the reaction mixture. During irradiation, the suspensions were exposed to air, but without additional aeration. Photo flux was measured using Radiometer (Cole Parmer, EW-97650-00) and it was 18.0 klx. After predetermined periods, aliquots were centrifuged for 10 min at the rate of 17,000 rpm and analyzed by UV-Vis spectrophotometry at 439 nm (Thermo Electron Corporation, Nicolet Evolution 500). The decolorization efficiency is then calculated as a difference between equilibrium concentration (at zero irradiation) and dye concentration after irradiation time t and expressed as $(C'_0 - C)/C'_0$, where C'_0 is the equilibrium concentration and C is dye concentration at irradiation time t , both given in mg/L.

Degree of mineralization was determined using a total organic carbon (TOC) analyzer (Shimadzu TOC 5050). A solution of 20 mg/L of azo-pyridone dye was prepared with the 1.0 g/L of TiO₂. Samples consisting of 4 mL aliquots were taken at different time intervals and centrifuged for 10 min at the rate of 17,000 rpm.

2.3. Experimental design and optimization by response surface methodology

In the present study, central composite design, which is a widely used form of RSM, was employed for the optimization of photocatalytic degradation of azo pyridone dye. A 2³ full factorial design is constructed in order to determine the effects of the main variables and the interactions between variables. A total of 17 experiments, including three replicates at the center point and six star points were performed. For statistical calculations, the variables X_i were coded as x_i according to the following relationship Eq. (1):

$$x_i = \frac{X_i - X_0}{\Delta x} \quad (1)$$

Table 1
Experimental range and level of the independent test variables ($\alpha = 1.682$)

Variable and designate	Coded values				
	$-\alpha$	-1	0	+1	$+\alpha$
H ₂ O ₂ concentration, X_1 [mg/L]	19.0	60.0	120.0	180.0	221.0
Irradiation time, X_2 [min]	15.0	25.0	40.0	55.0	65.0
TiO ₂ content, X_3 [g/L]	1.16	1.50	2.00	2.50	2.85

where x_i is the dimensionless coded value of each independent variable, X_0 is the value of X_i at the center point and Δx is the step change value [18]. Initial H₂O₂ concentration (X_1), irradiation time (X_2), and concentration of TiO₂ (X_3) were chosen as independent variables in this study. The response (Y) during all experimental designs was decolorization efficiency (%). Values of the independent variables and their variation limits were determined based on the related scientific literature and previous experimental results [7] and are presented in Table 1. Low and high levels are denoted as (-1) and (+1) respectively. Central points are denoted as 0, while star points are denoted as $+\alpha$ and $-\alpha$.

Experimental data were analyzed using Design Expert 8.0 software and fitted by a polynomial response equation. The following function, Eq. (2), was employed to attain the interaction between the dependent and independent variables:

$$Y = b_0 + \sum_{i=1}^k b_i X_i + \sum_{i=1}^k b_{ii} X_i^2 + \sum_{i=1}^k \sum_{j>1}^k b_{ij} X_i X_j + \sum_{i=1}^k \sum_{j>1}^k b_{ij} X_i X_j^2 \varepsilon \quad (2)$$

where Y is the predicted response; X_i, X_j, \dots, X_k are the input variables that affect the response; $Y, X_i^2, X_j^2, \dots, X_k^2$ are the square effects; $X_i X_j, X_i X_k, \dots, X_j X_k$, and $X_i X_j^2, X_i X_k^2, \dots, X_j X_k^2$ are the interaction effects; b_0 the intercept term; b_i is the linear term; b_{ii} is the square term; b_{ij} is the interaction term; and ε is a random error [19]. The quality of the fit of the polynomial model was expressed by the value of determination coefficient (R^2). The statistical significance was checked by F -test.

3. Results and discussion

3.1. Model fitting

It is well known that TiO₂ shows an excellent photocatalytic performance in azo dye degradation

[20,21]. In our previous study [7], the influence of various parameters on dye removal was investigated by classical univariate method using TiO₂ and simulated sunlight. In order to overcome the disadvantages of single-factor methodology, in this study, the influence of selected parameters was investigated by means of experimental design methodology. The results from previous work showed that H₂O₂, irradiation time, and TiO₂ content have great effects on photodegradation, and therefore, these variables were selected for process optimization. In addition, since photodegradation of aqueous organic pollutant is an electric-energy-intensive process, and electric energy can represent a major fraction of the operating costs, the investigation of the influence of irradiation time on decolorization efficiency is very useful for process economical feasibility.

Table 2 describes the factorial design of experiments, including the codified experimental values and observed and predicted decolorization efficiency. Central point experiments (denoted as 0) were repeated three times in order to check the reproducibility and obtain the standard deviation of the experimental response.

The obtained results indicate that the experimental values of dye degradation are very close to the predicted ones in all set of experiments. The highest

conversion of 98.69% and the lowest conversion of 54.12% were observed. One has to note that the highest and lowest conversions are obtained when values of independent variable X₂ (irradiation time) are positioned at star points.

By using the obtained experimental results, a regression model relating the response to the variables for the photocatalytic degradation of dye was developed. The relationship is given in the following polynomial equation, Eq. (3):

$$Y = 86.90 + 3.37X_1 + 12.35X_2 + 3.56X_3 + 1.29X_1X_2 - 2.01X_1^2 - 3.38X_2^2 - 3.94X_1X_2^2 \quad (3)$$

Table 3 shows the results of the response surface model fitting in the form of analysis of variance (ANOVA). ANOVA is required to test the significance and adequacy of the model [22]. Values of “Prob>F” less than 0.0500 indicate that the model is statistically significant. In addition, Fisher variation test, the F-value, which is a statistically valid measure of how well the factors describe the variations in the data about its mean, can be calculated from ANOVA. The greater the F-value is from unity, the more certain it is that the factors explain adequately the variation in the data about its mean, and that estimated factor effects are real.

High value for Fisher F test (F model = 96.47) and a very low probability value (P model > F = 0.0001) obtained in our study indicate that employed model is highly significant. In addition, the computed F-value is much greater than the tabular F value (F_{0.01 (14,15) tabular} = 5.61) at the 1% level, indicating that the treatment differences are highly significant.

The insights of model significance could be also obtained from determination coefficients. The determination coefficient (R²) quantitatively evaluates the correlation between the experimental data and the predicted responses. In this study, the high value of the determination coefficient is obtained (R² = 0.987), indicating that 98.7% of the result of the total variations can be explained by the suggested model. This also means that the model does not explain only about 1.3% of variation. In addition, high value for adjusted determination coefficient (adjusted R² = 0.977) define satisfactory adjustment of the polynomial model to the experimental data. The adjusted R² corrects the R² value for the sample size and the number of terms in the model. If there are many terms in the model and the sample size is not very large, the adjusted R² may be noticeably smaller than the R². Here, the adjusted R² is very close to the R² value [23].

Table 2
Full factorial central composite design matrix for three test variables, along with the observed and predicted responses

Run	X ₁	X ₂	X ₃	Decolorization efficiency [%]	
				Observed	Predicted
1	-1	1	-1	90.87	89.58
2	-1	-1	1	76.75	74.57
3	1	1	-1	92.43	91.03
4	-1	-1	-1	67.90	67.46
5	1	-1	1	72.86	70.87
6	1	-1	-1	64.38	63.76
7	1	1	1	96.82	98.15
8	-1	1	1	95.47	96.69
9	+α	0	0	85.94	86.89
10	-α	0	0	74.59	75.54
11	0	+α	0	98.69	98.12
12	0	-α	0	54.12	56.59
13	0	0	+α	91.76	92.89
14	0	0	-α	78.53	80.92
15	0	0	0	87.98	86.90
16	0	0	0	86.91	86.90
17	0	0	0	87.78	86.90

Table 3
Analysis of variance (ANOVA) of response surface model

Sources of variations	Sum of squares	d.f.	Mean square	F-value	Probability $P(>F)$
Model	2496.57	7	356.65	96.47 ^a	<0.0001
Residual	33.27	9	3.70		
Corrected total	2529.84	16			

$R^2 = 0.987$, adjusted $R^2 = 0.977$.

^a $F_{0.01(7,9)} = S_{p^2}/S_{e^2} = 96.47 \gg F_{0.01(7,9)tabular} = 5.61$.

Table 4
Regression results from the data of central composite design experiments

	Coefficient estimate	Standard error	95% confidence interval low	95% confidence interval high	t-value	p-value
Intercept	86.90	0.83	85.02	88.79	–	–
X_1	3.37	0.81	1.55	5.20	17.42	0.0024
X_2	12.35	0.52	11.17	13.53	563.34	<0.0001
X_3	3.56	0.52	2.38	4.73	46.74	<0.0001
X_1X_2	1.29	0.68	–0.25	2.83	3.59	0.0905
X_1^2	–2.01	0.55	–3.25	–0.77	13.52	0.0051
X_2^2	–3.38	0.55	–4.61	–2.14	38.09	0.0002
$X_1X_2^2$	–3.94	1.06	–6.33	–1.55	13.88	0.0047

3.2. Statistical analysis

Apart from the linear effect of the parameters on the response, the RSM also gives an insight into the quadratic and interaction effects of the parameters. The analysis of the various effects of the parameters is done by means of Fisher's 'F' test and Student 't' test. The Student 't' test is used to determine the significance of the regression coefficient of the parameters. The Fisher's F test is used to determine the significance of the interaction among the variables, which in turn may indicate the patterns of the mutual interactions between the test variables. In general, the larger the magnitude of the t-value and the smaller the value of p-probability, the more significant is the corresponding coefficient term [24]. The student t distribution and the corresponding p-values, along with the parameter estimate, were given in Table 4.

Considering only the first-order effect, the dye removal efficiency was improved at high H_2O_2 concentration (X_1), long irradiation times (X_2), and high TiO_2 content (X_3). According to parameter estimate and the corresponding p-values, the second two variables produce the largest effects on decolorization efficiency ($p < 0.0001$), while the effect of H_2O_2 concentration is less significant ($p = 0.0024$) in tested range.

H_2O_2 concentration has a positive synergistic effect when being coupled with irradiation time, which is

evident from the positive X_1X_2 terms in Eq. (1). This interaction does not influence the dye degradation significantly, due to the relatively high p value (p -value = 0.0905). However, the effects between H_2O_2 concentration and irradiation time are more significant when compared to those between each of these with TiO_2 content, which are statistically negligible for decolorization efficiency and are not included in Eq. (1).

Considering quadratic relations, a moderate quadratic effect for H_2O_2 concentration and high quadratic effect for irradiation time were observed ($p = 0.0051$ and 0.0002, respectively). p-value for (H_2O_2 concentration) (irradiation time)² was found to be 0.0047.

3.3. Effect of variables as response surface and counter plots

The 3D response surfaces plot and the 2D contour plot are generally the graphical representation of the regression equation. This representation shows the relative effects of any two variables when the remaining variable is kept constant.

To gain insights on the effect of each variable on response, it is helpful to look at the response plots in Fig. 1. Figure presents the influence of one variable on response, while other variables were kept constant at

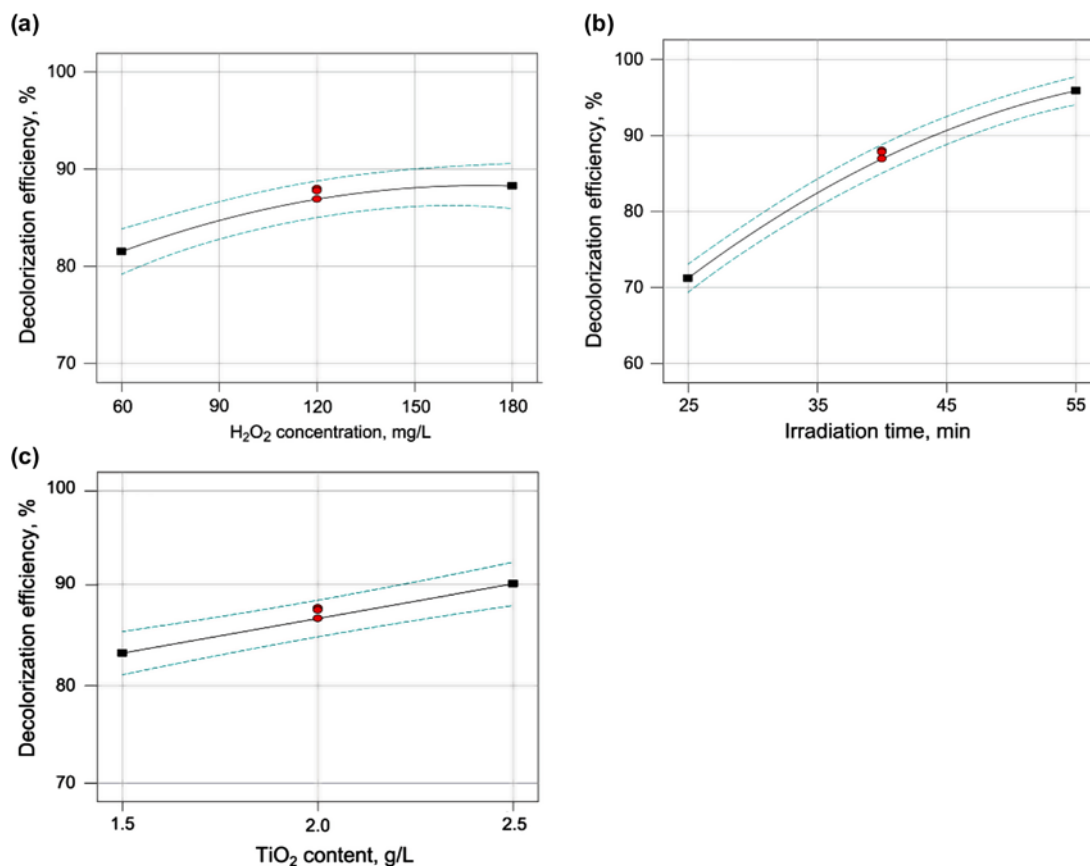


Fig. 1. Two factor interaction plots: (a) H₂O₂ concentration vs. decolorization efficiency (TiO₂ content: 2.00 g/L, irradiation time: 40.0 min), (b) irradiation time vs. decolorization efficiency (TiO₂ content: 2.00 g/L, H₂O₂ concentration: 120.0 mg/L), (c) TiO₂ content vs. decolorization efficiency (irradiation time: 40.0 min, H₂O₂ concentration: 120.0 mg/L).

their central level. Dotted lines represent the 95% confidence interval.

Investigation of H₂O₂ influence, Fig. 1(a), shows that increase in H₂O₂ concentration leads to increase in dye degradation up to certain level. Further increase beyond optimum H₂O₂ concentration does not influence decolorization efficiency or leads to decrease in decolorization. These findings are in agreement with other literature reports [25,26]. When present at low concentration, H₂O₂ acts as a source of hydroxyl radicals, and as an electron scavenger, thus inhibiting electron–hole recombination. Therefore, the increase in H₂O₂ concentration leads to increase in dye degradation. At one point, hydroxyl radicals reach equilibrium with H₂O₂. After this, when H₂O₂ is used in excess, hydroxyl radicals react with H₂O₂ and produce hydroxyperoxide radicals, which are less active than hydroxyl radicals. [21] Therefore, after a certain level of H₂O₂ has been exceeded, its further increase leads to decrease in decolorization. The various studies of photocatalytic degradation of azo dyes using TiO₂ and H₂O₂ are summarized in Table 5.

As expected, the decolorization efficiency increases with increase in irradiation time (Fig. 1(b)), since more and more dye molecules are being degraded during that time. However, the reaction rate decreases with irradiation time, since the reaction follows apparent first-order kinetics [7]. The figure shows that increasing the illumination time up to 50 min leads to a strong increase of dye degradation, but this increasing trend moderates, approaching an asymptotic plateau for $t > 50$ min. Additionally, this slow kinetics of dye degradation after a certain time may be due to active sites deactivation by strong by-products deposition.

The results concerning TiO₂ content show that increase in the TiO₂ content leads to increase in dye degradation (Fig. 1(c)). By increasing the TiO₂ content, the number of active sites increases and therefore the dye degradation increases. However, according to numerous studies, beyond a certain level of the TiO₂ concentration, the reaction rate decreases or becomes independent of the catalyst concentration [30]. This can be rationalized in terms of availability of active sites on TiO₂ surface and the light penetration into the

Table 5
Summary of photocatalytic degradation studies of azo dyes using TiO₂ and H₂O₂

Azo dye	Catalyst	Dye concentration (mg/L)	Optimal H ₂ O ₂ concentration (mg/L)	Reference
Cibacron Red FNR and Cibacron Yellow FN2R	TiO ₂ P-25 Degussa and TiO ₂ Hombikat UV-100	50	100	[27]
Auramine O	TiO ₂ P-25 Degussa, TiO ₂ -Rutile and ZnO	30		[28]
Gentian violet	TiO ₂ P-25 Degussa	73		[29]
Procion Red MX-5B	TiO ₂ P-25 Degussa	40	0.34	[30]
Remazol Red RR, Remazol Yellow RR, Procion Crimson H-EXL and Procion Yellow H-EXL	TiO ₂ P-25 Degussa	75	5000 (for Remazol Red RR)	[31]
Acid blue 74 (AB74)	TiO ₂ P-25 Degussa	11	3910	[32]
Methyl Orange	Pt-TiO ₂ /zeolite	20	40.8	[33]
Direct Red 23 (DR23)	Ag doped TiO ₂	163	340	[34]

suspension. Most of studies reported enhanced degradation rates for catalyst content up to 400–500 mg/L [29,35].

Information about interactions between irradiation time and H₂O₂ concentration can be obtained from the response and contour plots. In Fig. 2, the response surface and contour plot were developed as a function of H₂O₂ concentration and irradiation time, while TiO₂ content was kept constant at central level.

As can be seen from the contour plot (Fig. 2(b)), there is an increase in the degradation rate of dye with an increase of irradiation time, irrespective of

whether H₂O₂ concentration is at the low level or at high level. In addition, the decolorization efficiency increases with an increase of H₂O₂ concentration. However, increase in H₂O₂ concentration beyond optimal level does not have influence on decolorization efficiency or it leads to a slight decrease in decolorization efficiency.

The contour plot, Fig. 2(b) shows that when H₂O₂ concentration is in the range of (90–170) mg/L and irradiation time is in the range of (52–55) min, the decolorization efficiency of 95% is obtained (TiO₂ at central level).

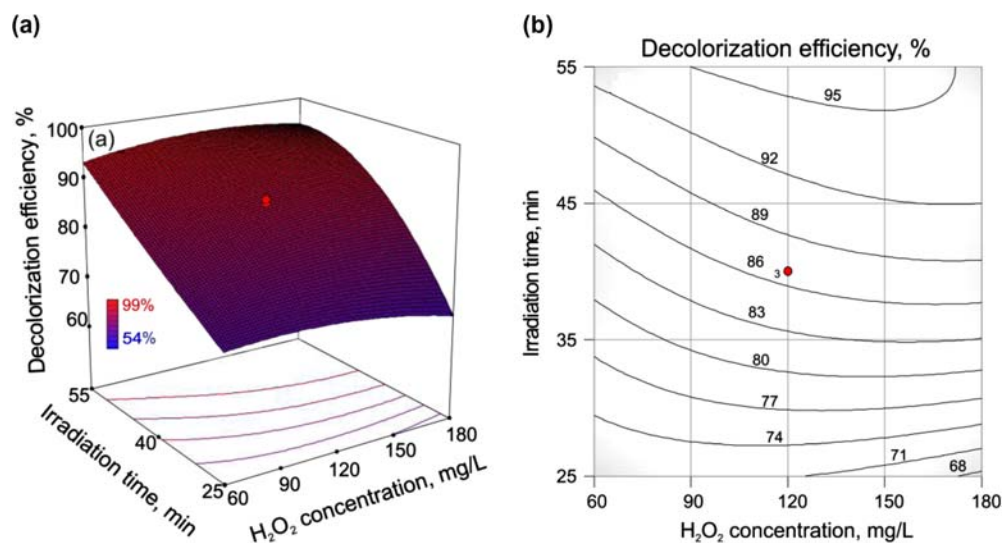


Fig. 2. The response surface plot (a) and contour plot (b) of photocatalytic decolorization efficiency as the function of H₂O₂ concentration and irradiation time; TiO₂ content: 2.00 g/L.

Table 6
The optimal values of variables for the maximum decolorization efficiency

H ₂ O ₂ concentration [mg/L]	<i>t</i> [min]	TiO ₂ content [g/L]	Predicted <i>Y</i> [%]	Experimental <i>Y</i> [%]
99.6	55.0	2.50	98.95	
120.9	55.0	2.30	98.00	
130.5	54.8	2.48	99.29	96.43
146.5	52.2	2.50	98.67	
155.0	55.0	2.50	99.17	
164.7	54.2	2.50	98.81	
170.0	55.0	2.50	98.64	
179.9	54.6	2.50	98.18	

3.4. Determination of optimal conditions for dye degradation

The main objective of the optimization in this work is to determine the optimum values of variables for photocatalytic degradation of dye by using model obtained from experimental data. After analyzing data with Design Expert software, the response optimizer program was used to calculate optimum conditions for maximizing the decolorization efficiency in the selected range of variables. Therefore, the response was chosen as to “maximize”, while process variables were selected to be “within the range”. Several combinations of the optimal values of variables are given in Table 6.

The maximum dye degradation is obtained for high TiO₂ content (>2.3 g/L), long irradiation time (>52 min), while optimal H₂O₂ concentration varied from (100–180) mg/L.

To confirm the model adequacy for predicting maximum degradation rate of azo pyridone dye, the model was validated by carrying out experiments using the following optimal conditions: H₂O₂ concentration: 130.5 mg/L; irradiation time: 54.8 min, and TiO₂ content: 2.48 g/L. Under these optimal conditions, the model predicted a maximum decolorization efficiency of 99.29%, while observed dye degradation was 96.43%. The difference between predicted and experimentally observed response is ~3% and the observed dye degradation is between low and high value of confidence intervals (94.43% and 104.17% respectively), indicating that the suggested model can be successfully applied for optimizing the studied process.

Although obtained model satisfactorily fits experimental data, the response confidence interval is quite wide and therefore, it is very difficult to predict 100% response. Irradiation time of 55 min and TiO₂ content

of 2.5 g/L are not sufficient for complete decolorization, which is sometimes required for wastewater treatment. In order to attain 100% decolorization efficiency, the irradiation time should be prolonged or TiO₂ content should be increased.

Fig. 3 shows 3D response surface plot, where response takes a value within the range between 94% and 100%, which corresponds to the magnitude of confidence interval. Table 6 shows optimum values of the process variables obtained for maximum decolorization efficiency of 100% (H₂O₂ concentration: 150.0 mg/L). The results indicate that complete decolorization could be achieved either by extended irradiation time to 58 min or by increasing TiO₂ content to 2.6 g/L.

3.5. Determination of operation cost

The main objective of RSM is to reduce the number of experiments to obtain optimal conditions for tested criteria and to determine possible interactions between variables. Nevertheless, results of RSM can be used for economic purposes. After finding several optimal options for maximum decolorization efficiency, it is favorable to investigate major fractions of the operating cost and to find the most economically feasible option.

The sum of personnel, maintenance materials, electricity, and chemical supplies presents the total operating cost of the photocatalytic process. The goal of RSM optimization in our study is to find maximum decolorization efficiency, by altering TiO₂ content, ini-

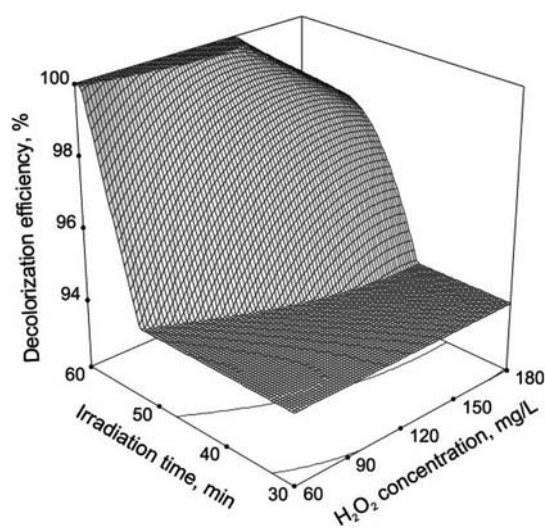


Fig. 3. The segment of response surface plot of photocatalytic decolorization efficiency (ranging from 94% to 100%); TiO₂: 2.50 g/L.

Table 7
Operation cost analysis for 100% decolorization efficiency

No.	TiO ₂ content [g/L]	<i>t</i> [min]	TiO ₂ cost/exp [€/exp]	Electrical energy [kW h]	Electrical energy cost [€/exp]	Σcost [€/exp]
A	2.50	58.2	0.0125	0.2912	0.0169	0.0294
B	2.60	55.0	0.0130	0.2750	0.0160	0.0290
C	2.70	51.9	0.0135	0.2596	0.0151	0.0286
D	2.80	49.8	0.0140	0.2492	0.0145	0.0285

tial H₂O₂ concentration, and irradiation time. Thus, the differences in operation cost for different optimized solutions come from: TiO₂ content, H₂O₂ consumption, and electrical energy. However, due to relatively low prices of H₂O₂, and due to low concentration used in this study, its effect on operation cost is negligible. Although TiO₂ could be recovered from wastewater systems by filtration/separation techniques, these techniques can be very tedious and expensive, especially when fine TiO₂ powders are used. Therefore, operation cost analysis is done by considering TiO₂ as a nonrecyclable component and only the effects of electrical energy consumption and TiO₂ amount on the overall operation cost will be determined.

At this point, one can note that large-scale power plants would probably exploit natural solar light, thus reducing the demand for electrical power. However, climatic conditions in most of the world's regions cannot provide continuous solar power needed for decomposition of pollutants from textile plants. Therefore, electrical energy consumption is also included in operation cost determination.

The operation costs for optimized solutions with different TiO₂ content and different irradiation times, labeled as A, B, C, and D, are calculated according to

Table 8
Decolorization and demineralization of dye during photocatalytic degradation (experimental conditions: TiO₂ content: 1.0 g/L, C₀: 20 mg/L, T: 25 °C)

Samples	C _{dye} [mg/L] ^a	C _{carbon} [mg/L] ^b	TOC [mg/L]
Original solution	20	8.74	8.76
Solution after adsorption	17.5	7.65	7.66
Solution after irradiation			
30 min	10.9	4.76	6.81
60 min	6.72	2.94	6.18
90 min	3.36	1.47	5.35
120 min	0.78	0.34	4.54
240 min	0	0	1.08

^aConcentration of dye.

^bConcentration of carbon in dye.

Eqs. (4) and (5), taking into account that the price of TiO₂ is 50.0 €/kg and the cost of electricity in Serbia is 0.058 €/kW h. It has to be pointed out that the costs shown in this study are approximate and are provided for illustrative purposes only. The light source was of 300 W and total volume was 100 mL. The TiO₂ and electric energy costs are calculated per experiment (€/exp) and the results are present in Tables 7 and 8.

$$\begin{aligned} \text{TiO}_2 \text{ cost (€/exp)} &= \text{TiO}_2 \text{ content (kg/L)} \\ &\quad \times \text{TiO}_2 \text{ cost (€/kg)} \\ &\quad \times \text{Volume (L)} \end{aligned} \quad (4)$$

$$\begin{aligned} \text{Electricenergy cost (€/exp)} \\ &= \text{Lamppower (kW)} \times \text{Irradiation time (h)} \\ &\quad \times \text{cost of electricity (€/kW h)} \end{aligned} \quad (5)$$

The obtained results show that the costs for TiO₂ and electrical energy consumption are of the same order of magnitude. However, the lowest operation cost is observed for the case D, where we noted decreased irradiation time and increased TiO₂ content relative to the other cases. This result indicates that the irradiation time represents a major fraction of the operation costs.

3.6. Dye mineralization

Since, the intermediate products of photocatalytic degradation of dye could be toxic, carcinogenic, and often more harmful to environmental than parental dye, complete decomposition to CO₂ is of great significance for process feasibility. Therefore, it is desirable to determine mineralization of dye. The extent of mineralization was studied by measuring total organic carbon (TOC) loss during photocatalytic degradation.

Results show that mineralization is a slower process than decolorization, requiring longer time for a complete TOC elimination. The kinetics of both processes followed first-order kinetics. After 140 min

of irradiation, total decolorization was reached, whereas 46% of TOC was removed by mineralization as shown in Tables 7 and 8. However, after 240 min, the TOC loss was larger than 90%, revealing that the dye could be efficiently demineralized using TiO₂ photocatalytic degradation.

4. Conclusions

The results of this study demonstrate that RSM could be efficiently used for the design and optimization of the photocatalytic degradation of azo pyridone dye. Analysis of variance showed a high coefficient of determination values ($R^2=0.987$ and adjusted $R^2=0.977$), thus ensuring a satisfactory adjustment of the regression model with the experimental data. The most significant effect on decolorization was found to be H₂O₂ concentration and irradiation time, while the influence of TiO₂ content was less important.

The model suggested that an average H₂O₂ concentration combined with increased TiO₂ content and high irradiation time would lead to maximum decolorization efficiency. Under selected optimal conditions (H₂O₂ concentration: 130.5 mg/L, irradiation time: 54.8 min, and TiO₂ content = 2.48 g/L) decolorization efficiency approached 96.43%. This experimental value was found to be in good agreement with the predicted one. Operation cost analysis showed that electrical energy consumption presents the major cost fraction. By using increased TiO₂ content, the electrical energy consumption needed for complete decolorization can be notably reduced, thus reducing total operation cost. TOC analysis showed that the azo pyridone dye could be effectively mineralized by TiO₂ photocatalytic process.

Acknowledgment

The authors gratefully acknowledge the funding by the Ministry of Education and Science of the Republic of Serbia, Project No. III 45001.

Symbols

x_i	— the dimensionless coded value of each independent variable
X_0	— the value of X_i at the center point
Δx	— the step change value
Y	— response
X_i, X_j, \dots, X_k	— the input variables that affect the response Y
$X_i^2, X_j^2, \dots, X_k^2$	— the square effects

$X_i X_j, X_i X_k, \dots, X_j X_k$	— the interaction effects
$X_i X_j^2, X_i X_k^2 \dots X_j X_k^2$	— the interaction effects
b_0	— the intercept term
b_i	— the linear terms
b_{ii}	— the square terms
b_{ij}	— the interaction terms
ε	— a random error
R^2	— determination coefficient

References

- [1] H. Zollinger, Color Chemistry: Synthesis, Properties and Applications of Organic Dyes and Pigments, Wiley-VCH, Weinheim, 2003.
- [2] R. Nilsson, R. Nordlinder, U. Wass, Asthma, rhinitis, and dermatitis in workers exposed to reactive dyes, *Brit. J. Ind. Med.* 50 (1993) 65–70.
- [3] B. Zohra, K. Aicha, S. Fatima, B. Nourredine, D. Zoubir, Adsorption of Direct Red 2 on bentonite modified by cetyltrimethylammonium bromide, *Chem. Eng. J.* 136 (2008) 295–305.
- [4] M. Riera-Torres, C. Gutiérrez-Bouzán, M. Crespi, Combination of coagulation-flocculation and nanofiltration techniques for dye removal and water reuse in textile effluents, *Desalination* 252 (2010) 53–59.
- [5] M. Kaneko, I. Okura, Photocatalysis Science and Technology, Kodansha Ltd., Tokyo, 2002.
- [6] I.K. Konstantinou, T.A. Albanis, TiO₂-assisted photocatalytic degradation of azo dyes in aqueous solution: kinetics and mechanistic investigations. A review, *Appl. Catal., B* 49 (2004) 1–4.
- [7] J. Dostanić, D. Lončarević, P. Banković, O. Cvetković, D. Jovanović, D. Mijin, Influence of process parameters on the photodegradation of synthesized azo pyridone dye in TiO₂ water suspension under simulated sunlight, *J. Environ. Sci. Health, Part A: Toxic/Hazard. Subst. Environ. Eng.* 46 (2011) 70–79.
- [8] Y.L. Song, J.T. Li, B. Bai, TiO₂-assisted photodegradation of Direct Blue 78 in aqueous solution in sunlight, *Water Air Soil Pollut.* 213 (2010) 311–317.
- [9] A.P. Toor, A. Verma, C.K. Jotshi, P.K. Bajpai, V. Singh, Photocatalytic degradation of Direct Yellow 12 dye using UV/TiO₂ in a shallow pond slurry reactor, *Dyes Pigm.* 68 (2006) 53–60.
- [10] P. Pichat, C. Guillard, L. Amalric, A.-C. Renard, O. Plaidy, Assessment of the importance of the role of H₂O₂ and O²⁻ in the photocatalytic degradation of 1,2-dimethoxybenzene, *Solar Energy Mater. Solar Cells* 38 (1995) 391–399.
- [11] K. Tanaka, T. Hisanaga, K. Harada, Photocatalytic degradation of organohalide compounds in semiconductor suspension with added hydrogen peroxide, *New J. Chem.* 13 (1989) 5–7.
- [12] N. Daneshvar, D. Salari, A.R. Khataee, Photocatalytic degradation of azo dye acid red 14 in water: investigation of the effect of operational parameters, *J. Photochem. Photobiol. A: Chem.* 157 (2003) 111–116.
- [13] C. Betianu, F.A. Caliman, M. Gavrilescu, I. Cretescu, C. Cojocaru, I. Poulios, Response surface methodology applied for Orange II photocatalytic degradation in TiO₂ aqueous suspension, *J. Chem. Technol. Biotechnol.* 83 (2008) 1454–1465.
- [14] Z. Alam, S.A. Muyibi, J. Toramae, Statistical optimization of adsorption processes for removal of 2,4-dichlorophenol by activated carbon derived from oil palm empty fruit bunches, *J. Environ. Sci.* 19 (2007) 674–677.
- [15] R.H. Myers, D.C. Montgomery, Response Surface Methodology, Wiley, New York, NY, 2002.
- [16] R. Priya, S. Kanmani, Optimization of photocatalytic production of hydrogen from hydrogen sulfide in alkaline solution using response surface methodology, *Desalination* 276 (2011) 222–227.

- [17] A.F. Caliman, C. Cojocaru, A. Antoniadis, I. Poulios, Optimized photocatalytic degradation of Alcian Blue 8 GX in the presence of TiO₂ suspensions, *J. Hazard. Mater.* 144 (2007) 265–273.
- [18] A.R. Khatee, Optimization of UV-promoted peroxydisulphate oxidation of C.I. Basic Blue 3 using response surface methodology, *Environ. Technol.* 31 (2010) 73–86.
- [19] Ž. Lazić, *Design of Experiments in Chemical Engineering*, Wiley-VCH, Weinheim, 2004.
- [20] D. Gumus, F. Akbal, Photocatalytic degradation of textile dye and wastewater, *Water Air Soil Pollut.* 216 (2011) 117–124.
- [21] M.A. Rauf, M.A. Meetani, S. Hisaindee, An overview on the photocatalytic degradation of azo dyes in the presence of TiO₂ doped with selective transition metals, *Desalination* 276 (2011) 13–27.
- [22] S. Akhnazarova, V. Kafarov, *Experiment Optimization in Chemistry and Chemical Engineering*, MIR Publisher, Moscow, 1982.
- [23] S.C.R. Santos, R.A.R. Boaventura, Adsorption modeling of textile dyes by sepiolite, *Appl. Clay Sci.* 42 (2008) 137–145.
- [24] M. Zarei, D. Salari, A. Niaei, A.R. Khataee, Application of response surface methodology for optimization of peroxi-coagulation of textile dye solution using carbon nanotube-PTFE cathode, *J. Hazard. Mater.* 173 (2010) 544–551.
- [25] L. Andronic, A. Duta, Influence of pH and H₂O₂ on dyes photodegradation, *Phys. Status Solidi C* 5 (2008) 3332–3337.
- [26] C. Galindo, P. Jacques, A. Kalt, Photodegradation of the aminoazobenzene acid orange 52 by three advanced oxidation processes: UV/H₂O₂, UV/TiO₂ and VIS/TiO₂: comparative mechanistic and kinetic investigations, *J. Photochem. Photobiol. A* 130 (2000) 35–47.
- [27] E. Bizani, K. Fytianos, I. Poulios, V. Tsiridis, Photocatalytic decolorization and degradation of dye solutions and wastewaters in the presence of titanium dioxide, *J. Hazard. Mater.* 136 (2006) 85–94.
- [28] I. Poulios, A. Avranas, E. Rekliti, A. Zouboulis, Photocatalytic oxidation of Auramine O in the presence of semiconducting oxides, *J. Chem. Technol. Biotechnol.* 75 (2000) 205–212.
- [29] M. Saquib, M. Muneer, TiO₂-mediated photocatalytic degradation of a triphenylmethane dye (gentian violet), in aqueous suspensions, *Dyes Pigm.* 56 (2003) 37–49.
- [30] C.M. So, M.Y. Cheng, J.C. Yu, P.K. Wong, Degradation of azo dye Procion Red MX-5B by photocatalytic oxidation, *Chemosphere* 46 (2002) 905–912.
- [31] K. Soutsas, V. Karayannis, I. Poulios, A. Riga, K. Ntampeglitis, X. Spiliotis, G. Papapolymerou, Decolorization and degradation of reactive azo dyes via heterogeneous photocatalytic processes, *Desalination* 250 (2010) 345–350.
- [32] Catherine Galindo, Patrice Jacques, André Kalt, Photochemical and photocatalytic degradation of an indigoid dye: a case study of acid blue 74 (AB74), *J. Photochem. Photobiol. A* 141 (2001) 47–56.
- [33] Miaoliang Huang, Chunfang Xu, Zibao Wu, Yunfang Huang, Jianming Lin, Jihuai Wu, Photocatalytic discolorization of methyl orange solution by Pt modified TiO₂ loaded on natural zeolite, *Dyes Pigm.* 77 (2008) 327–334.
- [34] N. Sobana, K. Selvam, M. Swaminathan, Optimization of photocatalytic degradation conditions of Direct Red 23 using nano-Ag doped TiO₂, *Sep. Purif. Technol.* 62 (2008) 648–653.
- [35] J. Grzechulska, A.W. Morawski, Photocatalytic decomposition of azo-dye acid black 1 in water over modified titanium dioxide, *Appl. Catal. B* 36 (2002) 45–51.